Table 1　GCC-LC/MS を用いた PA 単糖分析における PA 糖鎖安定同位体の影響

	SIM ion intensity (peak area ratio %) derived from d_0-PA and d_4-PA-monosaccharides											
Ion (*m/z*)	d_0PA-Fuc	d_4PA-Fuc	d_0PA-Gal	d_4PA-Gal	d_0PA-Man	d_4PA-Man	d_0PA-Glc	d_4PA-Glc	d_0PA-GlcNAc	d_4PA-GlcNAc	d_0PA-GalNAc	d_4PA-GalNAc
243	86.6	-										
244	11.7	-										
245	1.7	0.7										
246	-	4.6										
247	-	82.6										
248	-	10.4										
249	-	1.7										
259			87.4	-	88.6	-	87.6	-				
260			11.0	-	9.9	-	11.1	-				
261			1.6	0.7	1.5	0.4	1.3	0.8				
262			-	4.1	-	2.9	-	4.1				
263			-	83.1	-	78.7	-	79.3				
264			-	10.5	-	14.4	-	13.4				
265			-	1.6	-	3.6	-	2.4				
300									86.0	-	85.5	-
301									12.3	-	12.9	-
302									1.7	0.4	1.6	0.5
303									-	4.1	-	4.6
304									-	81.0	-	81.1
305									-	12.5	-	12.0
306									-	2.0	-	1.8

10 pmol PA or d_4PA-monosaccharide was injected

Table 2

内部標準単糖を用いた GCC-LC/MS による d_0-PA-単糖分析の再現性(RSD)

	d_0-PA-monosaccharides (pmol)								
	0.05			0.5			5		
	IS(-)	IS(A)	IS(B)	IS(-)	IS(A)	IS(B)	IS(-)	IS(A)	IS(B)
Gal	16.2	15.5	5.7	11.6	8.3	2.1	5.0	5.5	2.3
Man	12.7	15.3	4.7	9.7	7.1	1.8	7.2	4.6	1.7
Glc	12.9	17.5	3.9	8.9	7.6	4.8	10.9	5.1	1.1
Fuc	23.9	17.3	4.2	9.9	7.6	1.9	5.4	6.1	0.8
GlcNAc	15.2	7.7	3.5	9.0	5.6	2.0	5.4	6.0	1.2
GalNAc	16.0	21.0	9.4	11.4	7.4	4.7	9.8	3.5	1.5

Note. n=5. IS, internal standard. A, PA-rhmnose; B, d_4-PA-monosaccharides.

Table 3

内部標準単糖を用いた GCC-LC/MS による単糖組成分析

Glycoprotein	Monosaccharide	mol/mol[a]	mol/mol
Fetuin	Fuc	0.3	0[b]
	Gal	10.4	12
	Man	7.6	9
	GlcNAc	14.7	15
	GalNAc	3.4	3
Erythropoietin	Fuc	3.4	4.1[c]
	Gal	12.8	13.8
	Man	8.1	8.7
	GlcNAc	15.6	17.2
	GalNAc	1.5	0.9

[a]Values were expressed as mol detected in 1 mol glycoprotein. [b]Ref , *Anal. Biochem.* 197, (1991) 132-136; [c]Ref , *J. Biol. Chem.* 262 (1987) 12059-12076

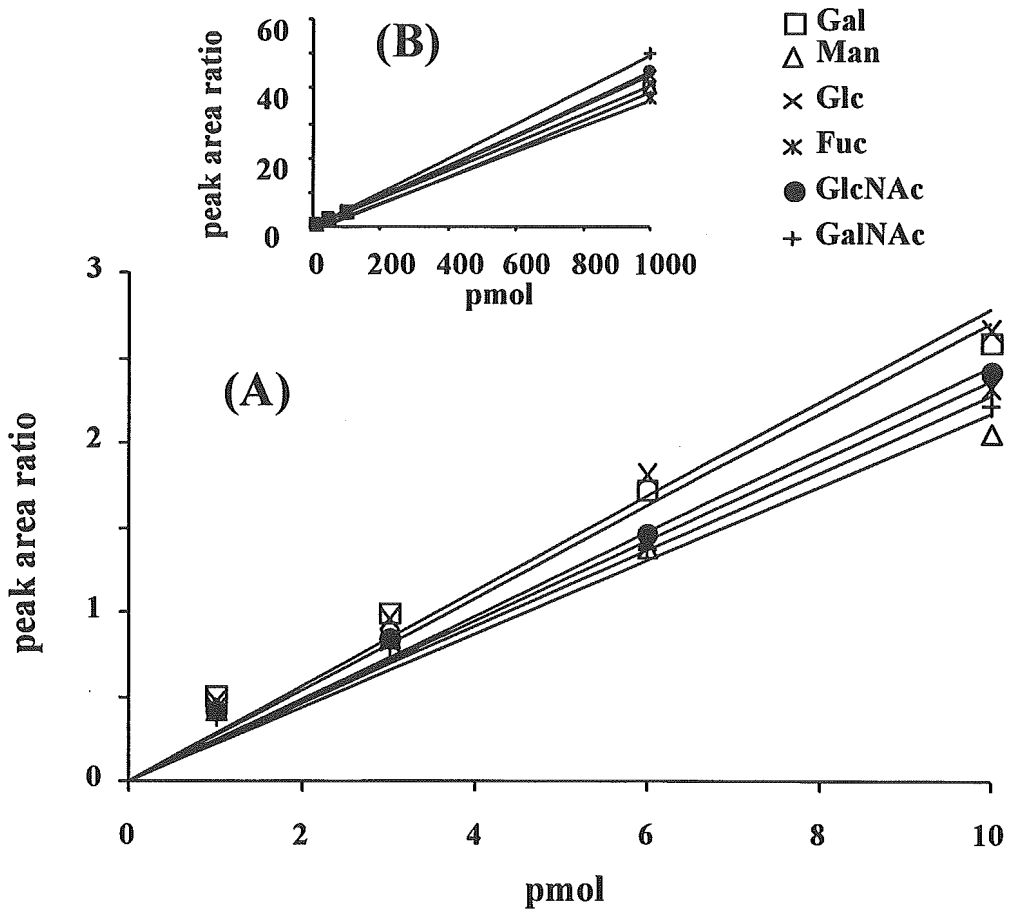

Fig. 3 安定同位体標識単糖及びGCC-LC/MSを用いた単糖分析法の定量性

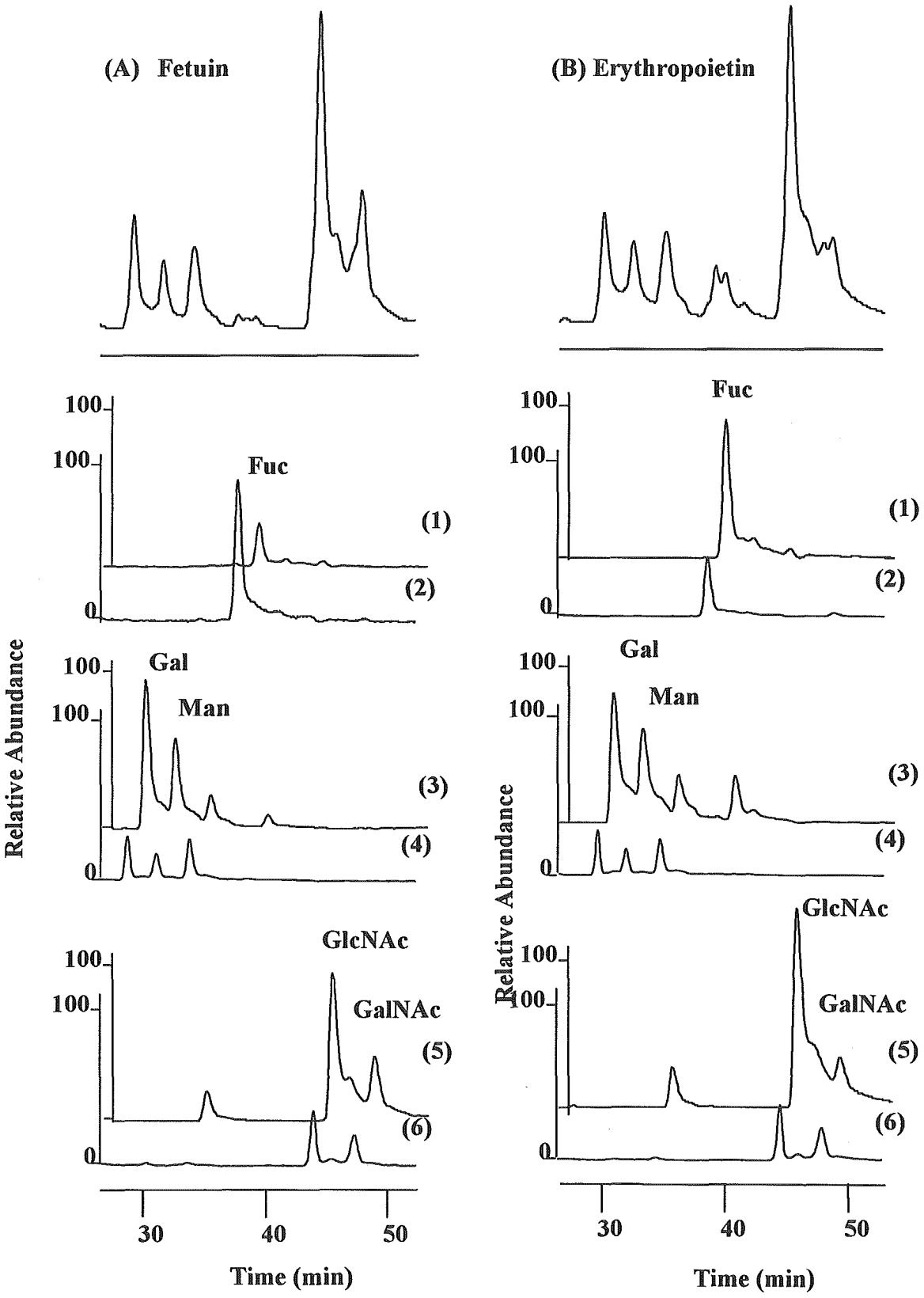

Fig. 4 フェツイン(A)及びエリスロポエチン(B)の単糖組成分析

マスクロマトグラム *m/z* 243 (1), 247 (2), 259 (3), 263 (4), 300 (5), 304 (6)

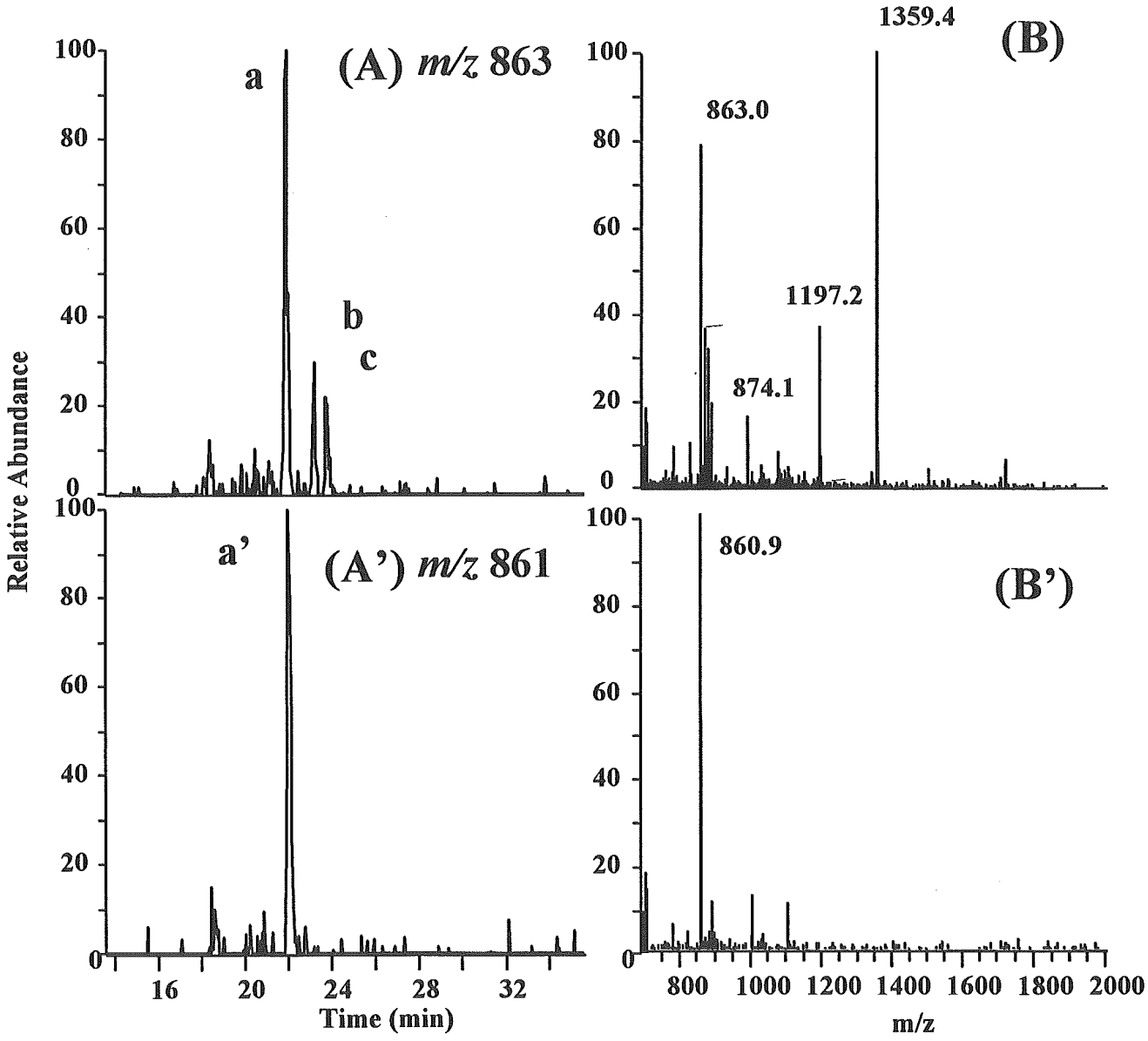

Fig. 5　hCG由来d_4-PA化アシアロ２本鎖糖鎖のGCC-LC/MS

(A), (A'), マスクロマトグラム; ピークa、a'のマススペクトル(B), (B')
(A), (B), positive ion mode; (A'), (B'), negative ion mode

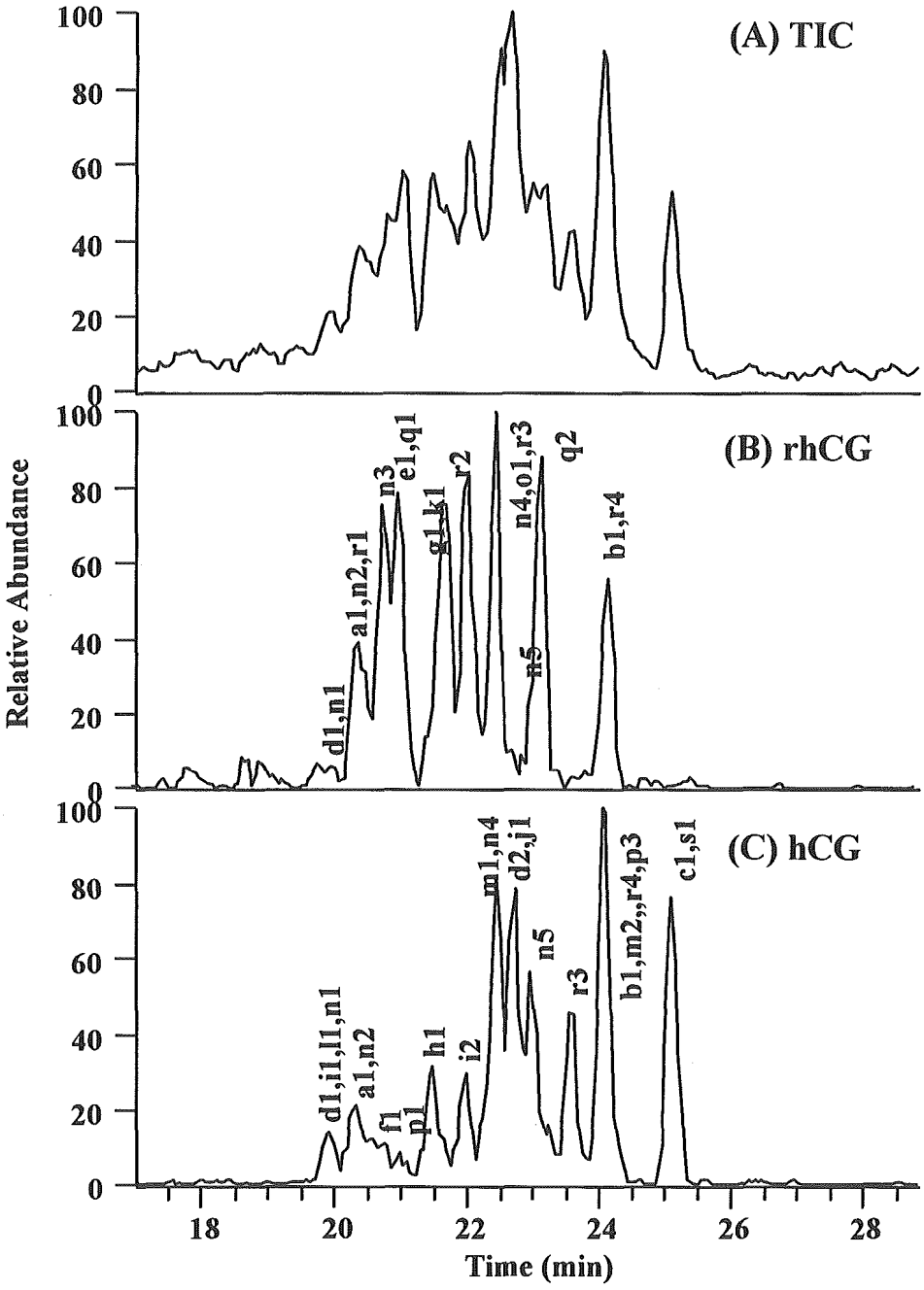

Fig. 6 PA化hCG由来糖鎖のプロファイル

(A), d_4-PA hCG 及び d_0-PA rhCG 混合物のTIC; (B), d_4-PA hCGのTIC; (C), d_0-PA rhCG のTIC

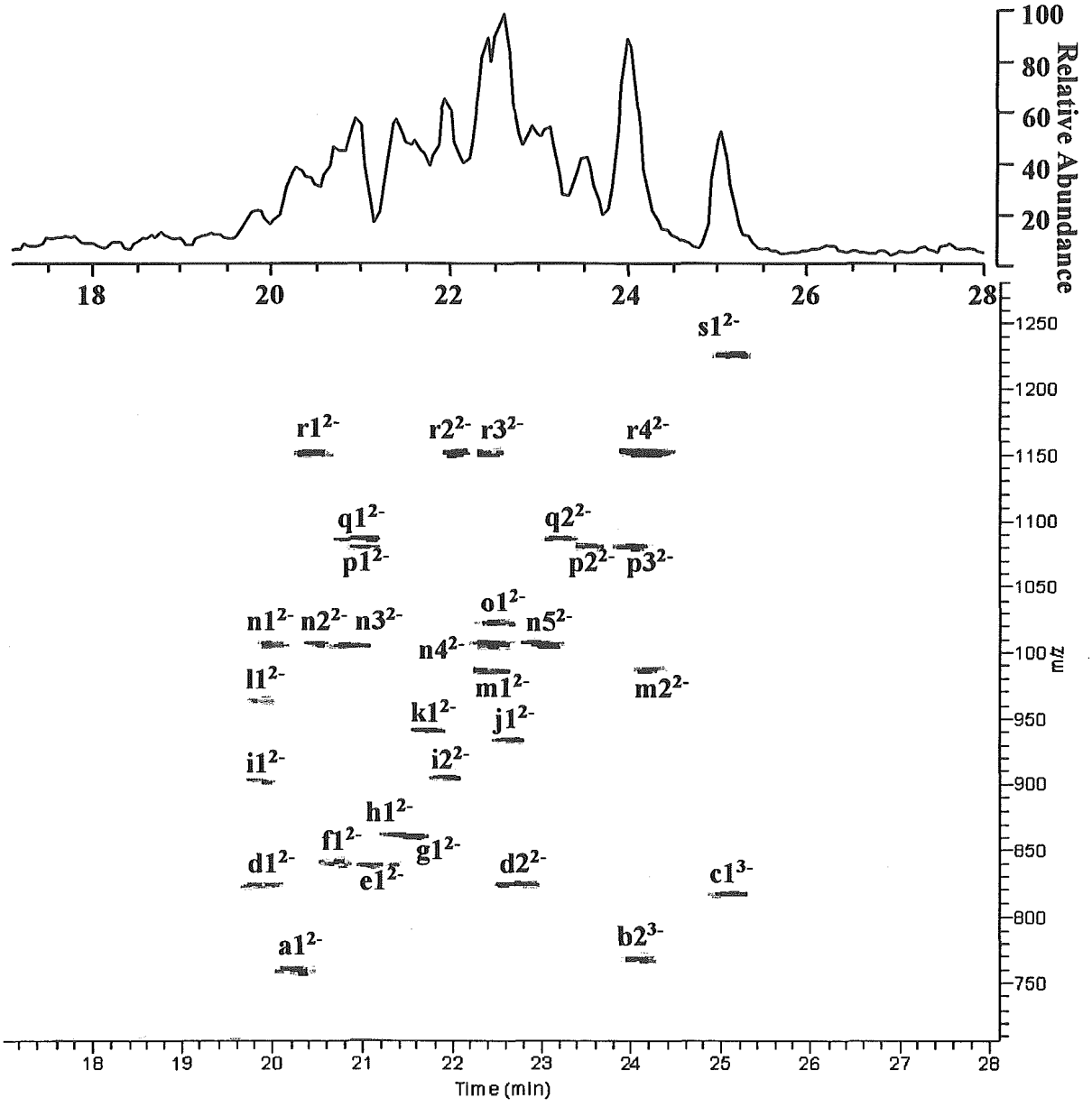

Fig. 7　d_0-PA rhCG 及び d_4-PA hCG 混合物のTICの2D表示

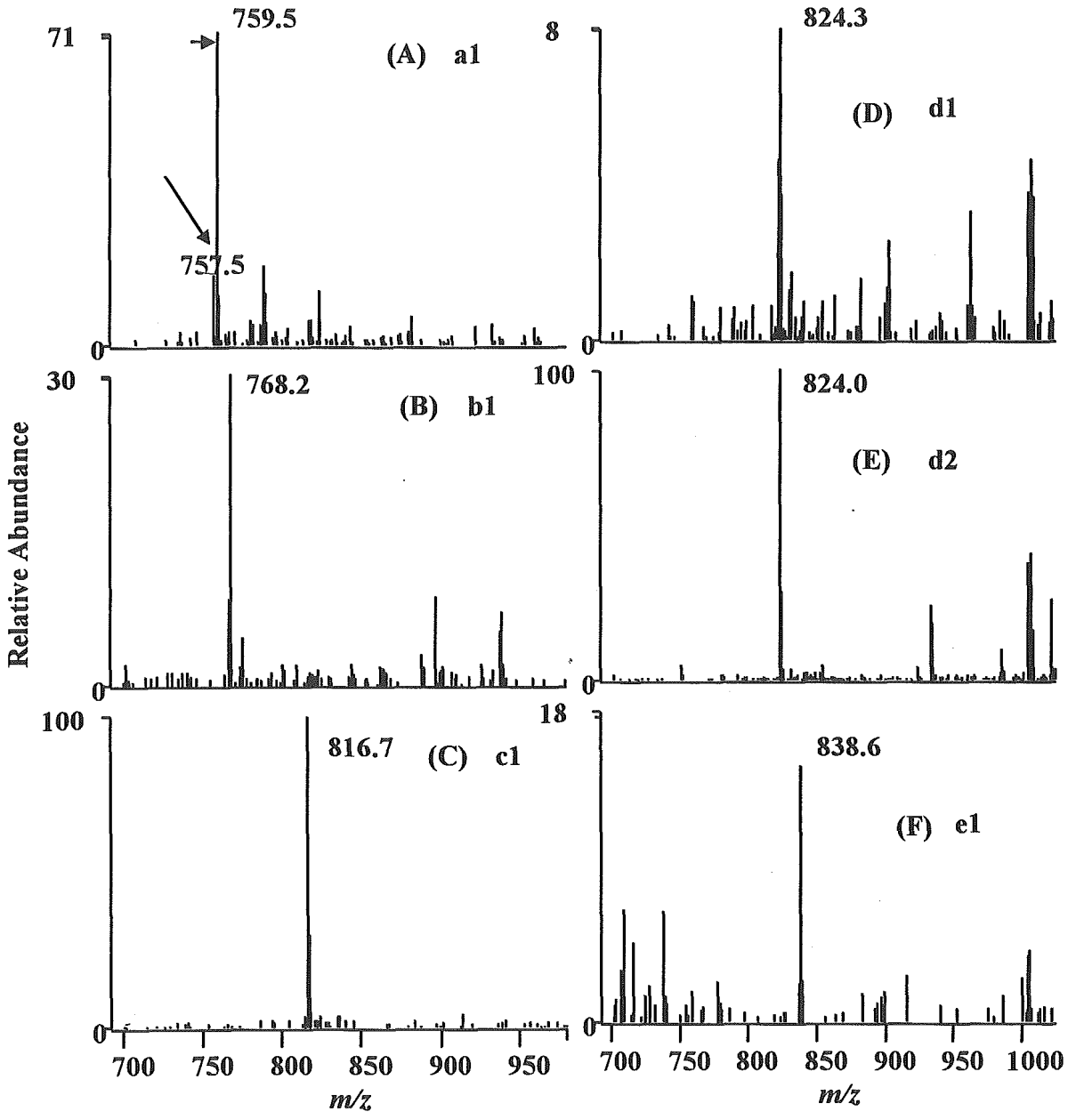

Fig. 8-1　Fig. 7中のピーク a~s のマススペクトル

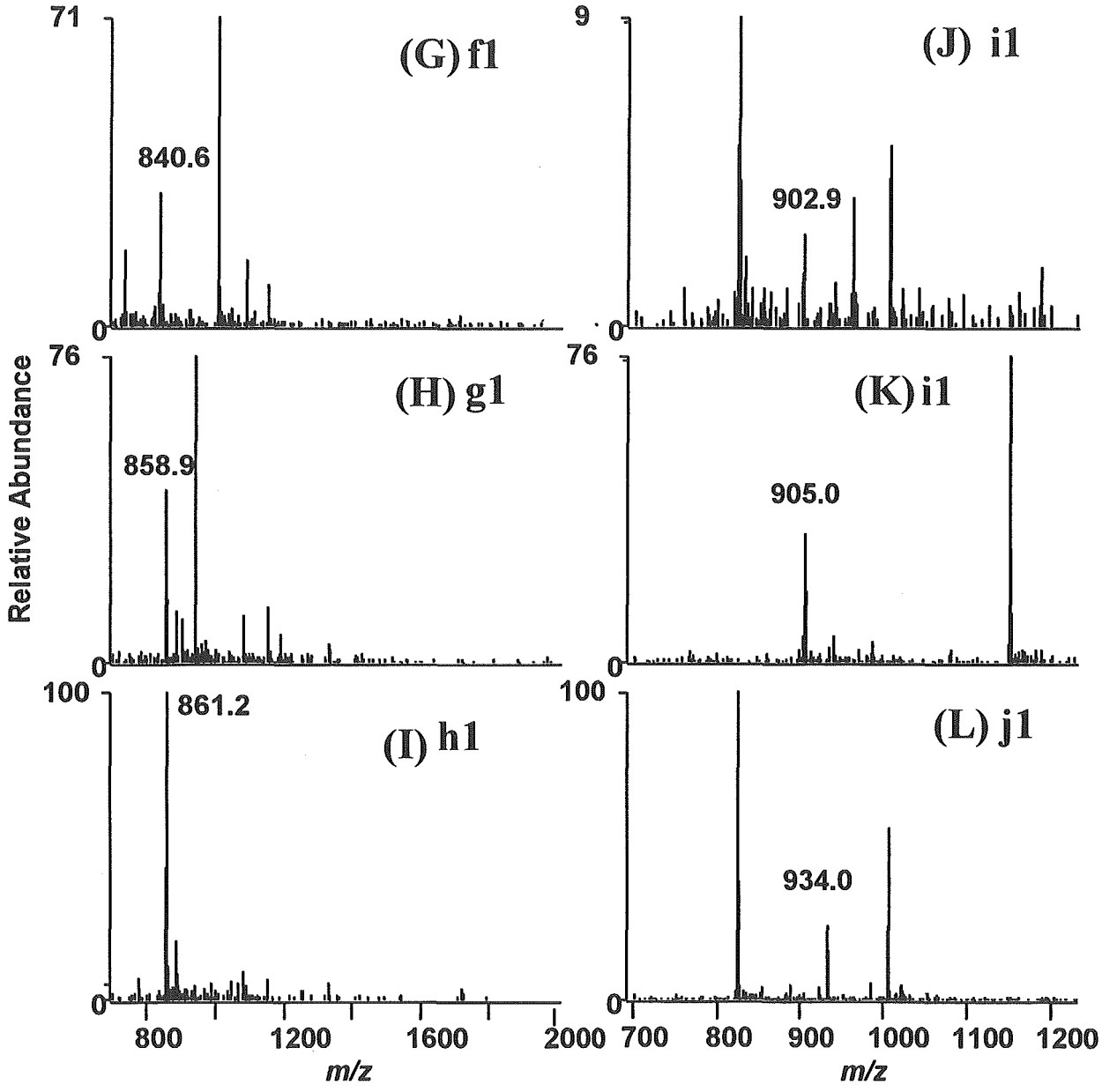
71
(G) f1
840.6
0
9
(J) i1
902.9
0
76
(H) g1
858.9
0
76
(K) i1
905.0
0
Relative Abundance
100
861.2
(I) h1
0
100
(L) j1
934.0
0
800
1200
1600
2000
m/z
700
800
900
1000
1100
1200
m/z

Fig. 8-2　つづき

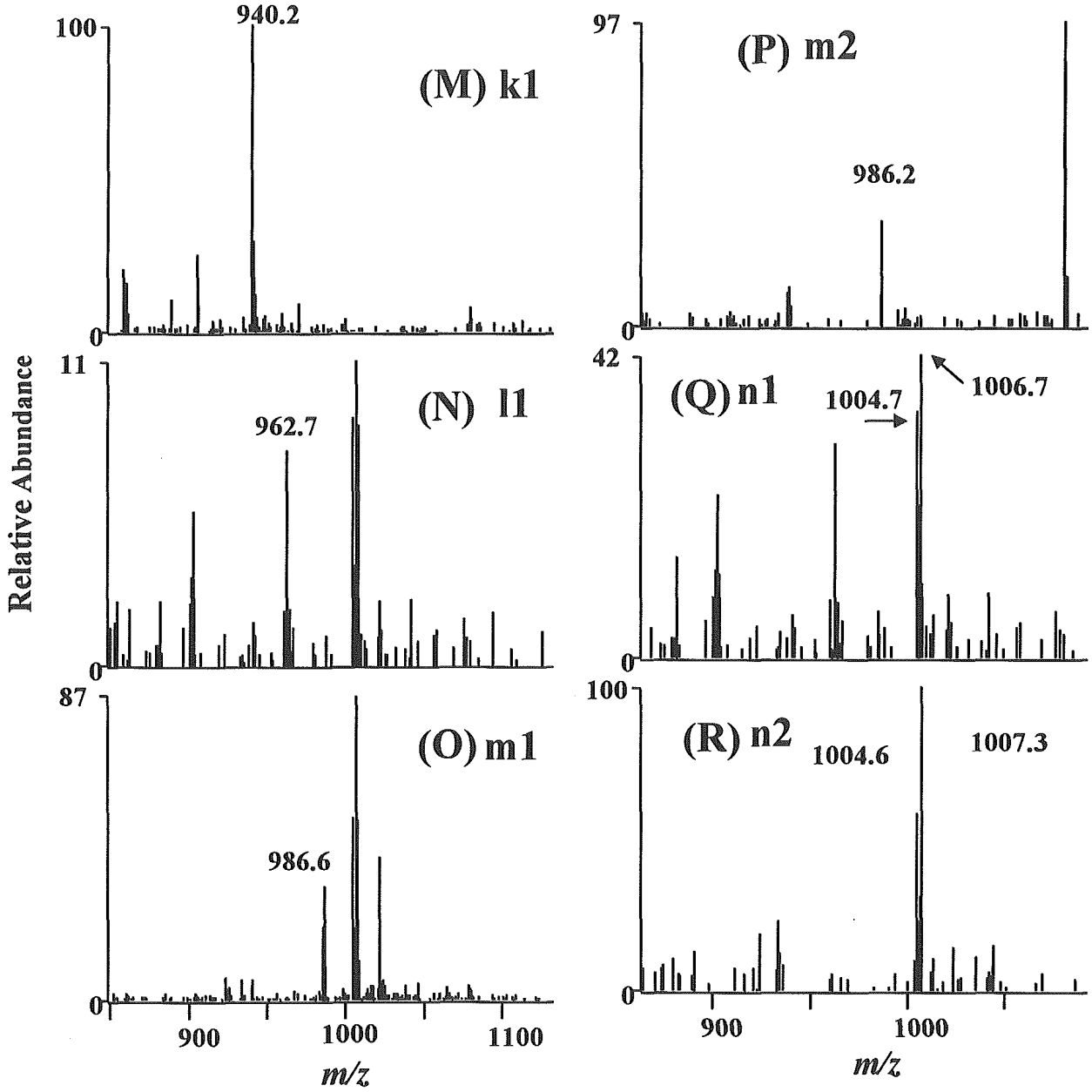
100
940.2
(M) k1
0
97
(P) m2
986.2
0
11
962.7
(N) l1
0
42
(Q) n1
1004.7
1006.7
0
87
(O) m1
986.6
0
100
(R) n2
1004.6
1007.3
0
900
1000
1100
m/z
900
1000
m/z
Relative Abundance

Fig. 8-3　つづき

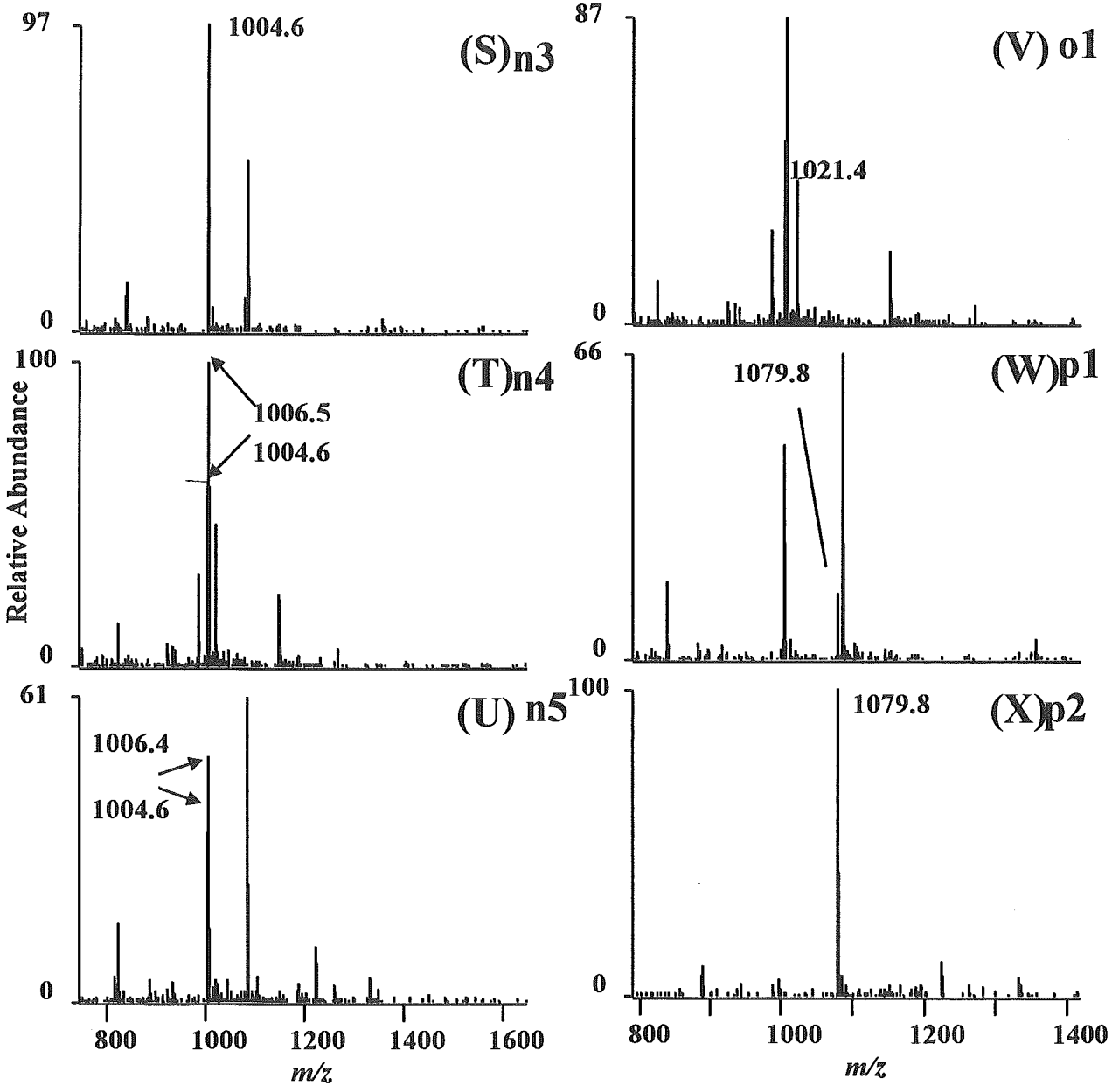
97
1004.6
(S)n3
0
87
(V) o1
1021.4
0
100
(T)n4
1006.5
1004.6
0
66
1079.8
(W)p1
0
61
(U) n5
1006.4
1004.6
0
100
1079.8
(X)p2
0
Relative Abundance
800
1000
1200
1400
1600
m/z
800
1000
1200
1400
m/z

Fig. 8-4　つづき

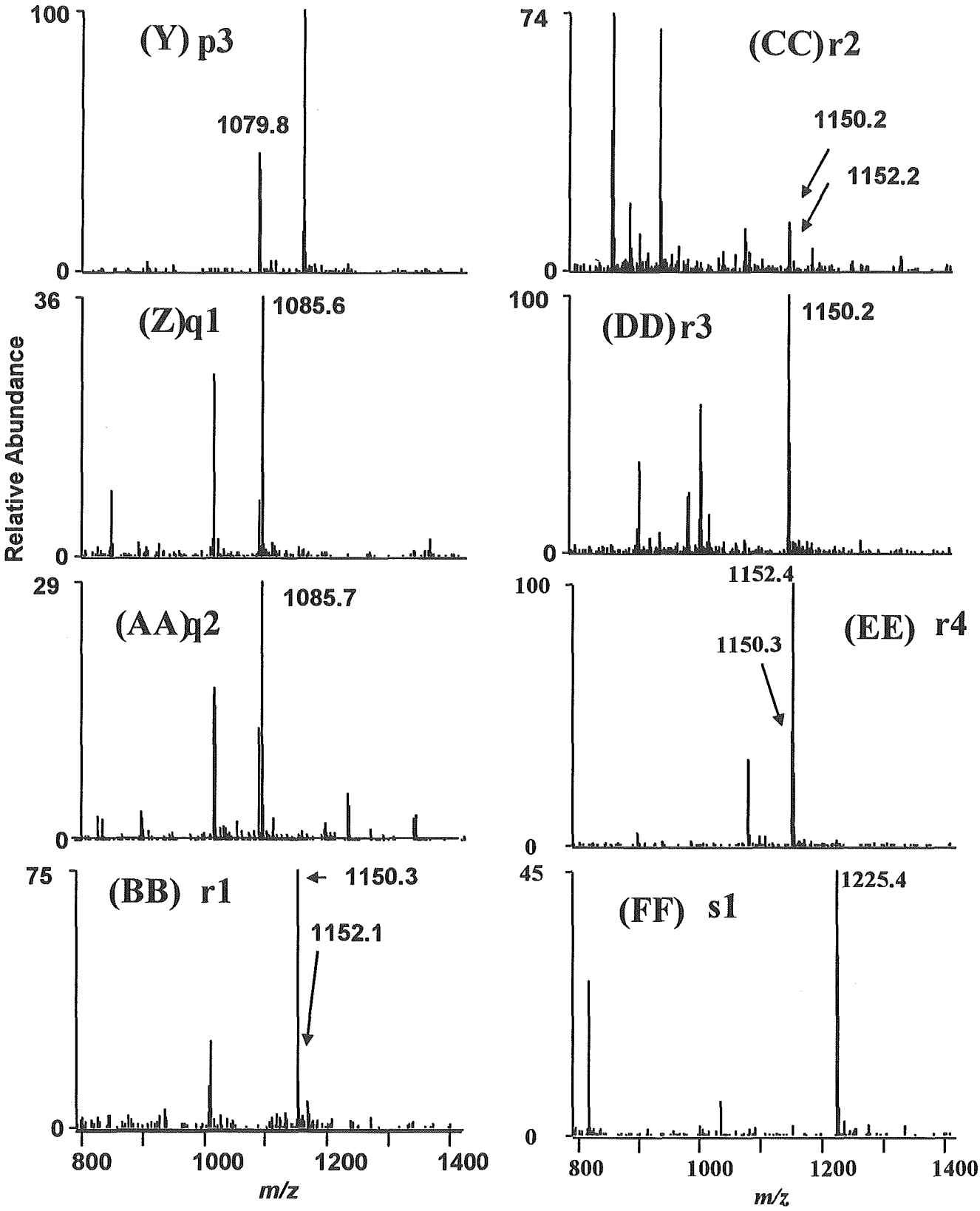
Relative Abundance
100
(Y) p3
1079.8
0
74
(CC) r2
1150.2
1152.2
0
36
(Z)q1
1085.6
0
100
(DD) r3
1150.2
0
29
(AA)q2
1085.7
0
100
1152.4
1150.3
(EE) r4
0
75
(BB) r1
1150.3
1152.1
0
45
(FF) s1
1225.4
0
800
1000
1200
1400
m/z
800
1000
1200
1400
m/z

Fig. 8-5　つづき

Table 4　Fig. 7 で検出されたピーク a-s の帰属

Peak No.	Carbohydrate composition	Deduced structure	Theoretical mass (d_0PA-sugar)	Observed *m/z*		
				d_0-PA rhCG	d_4-PA hCG	
				M^{2-}	M^{3-}	M^{2-}
a1	$[Hex]_5[HexNAc]_3$	Hybrid(1)	1517.5	757.5		759.5
b1	$[Hex]_5[HexNAc]_4[NeuNAc]_2$	Bi(1)NA_2	2303.1		768.2	
c1	$[Fuc]_1[Hex]_5[HexNAc]_4[NeuNAc]_2$	FBi(1)NA_2	2449.3		816.7	
d1	$[Hex]_4[HexNAc]_3[NeuNAc]_1$	Mono(1)NA	1646.6			824.3
d2	$[Hex]_4[HexNAc]_3[NeuNAc]_1$	Mono(1)NA	1646.6			824.0
e1	$[Hex]_6[HexNAc]_3$	Hybrid(2)	1679.6	838.6		
f1	$[Hex]_6[HexNAc]_3$	Hybrid(2)	1679.6			840.6
g1	$[Hex]_5[HexNAc]_4$	Bi(1)	1720.7	858.9		
h1	$[Hex]_5[HexNAc]_4$	Bi(1)	1720.7			861.2
i1	$[Hex]_5[HexNAc]_3[NeuNAc]_1$	Hybrid(1)NA	1807.7	902.9		
i2	$[Hex]_5[HexNAc]_3[NeuNAc]_1$	Hybrid(1)NA	1808.7			905.0
j1	$[Fuc]_1[Hex]_5[HexNAc]_4$	FBi(1)	1866.8			934.0
k1	$[Hex]_6[HexNAc]_4$	Hybrid(3)	1882.8	940.2		
l1	$[Hex]_5[HexNAc]_5$	Bi(1)-GN	1924.9			962.7
m1	$[Hex]_6[HexNAc]_3[NeuNAc]_1$	Hybrid(2)NA	1970.8			986.8
m2	$[Hex]_6[HexNAc]_3[NeuNAc]_1$	Hybrid(2)NA	1970.8			986.2
n1	$[Hex]_5[HexNAc]_4[NeuNAc]_1$	Bi(1)NA	2011.9	1004.7		1006.7
n2	$[Hex]_5[HexNAc]_4[NeuNAc]_1$	Bi(1)NA	2011.9	1004.6		1007.3
n3	$[Hex]_5[HexNAc]_4[NeuNAc]_1$	Bi(1)NA	2011.9	1004.6		
n4	$[Hex]_5[HexNAc]_4[NeuNAc]_1$	Bi(1)NA	2011.9	1004.6		1006.5
n5	$[Hex]_5[HexNAc]_4[NeuNAc]_1$	Bi(1)NA	2011.9	1004.6		1006.4
o1	$[Hex]_7[HexNAc]_4$	Hybrid(4)	2044.9	1021.4		
p1	$[Fuc]_1[Hex]_5[HexNAc]_4[NeuNAc]_1$	FBi(1)NA	2158.0			1079.8
p2	$[Fuc]_1[Hex]_5[HexNAc]_4[NeuNAc]_1$	FBi(1)NA	2158.0			1079.8
p3	$[Fuc]_1[Hex]_5[HexNAc]_4[NeuNAc]_1$	FBi(1)NA	2158.0			1079.8
q1	$[Hex]_6[HexNAc]_4[NeuNAc]_1$	Hybrid(3)NA	2174.0	1085.6		
q2	$[Hex]_6[HexNAc]_4[NeuNAc]_1$	Hybrid(3)NA	2174.0	1085.7		
r1	$[Hex]_5[HexNAc]_4[NeuNAc]_2$	Bi(1)NA_2	2303.1	1150.3		1152.1
r2	$[Hex]_5[HexNAc]_4[NeuNAc]_2$	Bi(1)NA_2	2303.1	1150.2		1152.2
r3	$[Hex]_5[HexNAc]_4[NeuNAc]_2$	Bi(1)NA_2	2303.1	1150.1		
r4	$[Hex]_5[HexNAc]_4[NeuNAc]_2$	Bi(1)NA_2	2303.1	1150.3		1152.4
s1	$[Fuc]_1[Hex]_5[HexNAc]_4[NeuNAc]_2$	FBi(1)NA_2	2449.3			1225.4

Hex: hexsose, HexNAc: *N*-acetyl hexsosamine, NeuNAc, NA: *N*-acetyl neuraminic acid, Fuc, F: fucose, mono: monoantennary, bi: biantennary, GN: bisecting GlcNAc

Table 5　Table 4 に示した糖鎖の推定構造

Abbreviation	Structure [a]	Theoretical mass [b]
Hybrid(1)	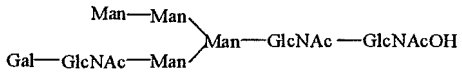	1440.3
Hybrid(2)	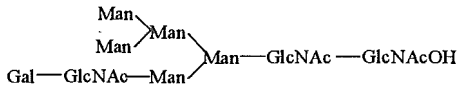	1602.5
Hybrid(3)	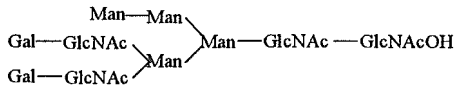	1440.3
Hybrid(4)	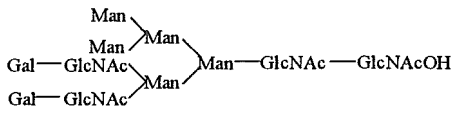	1805.6
Mono(1)	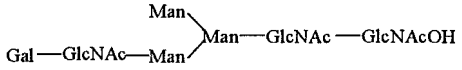	1278.2
Bi(1)	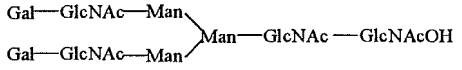	1643.5
Bi(1)-GN	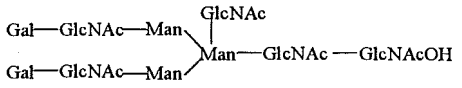	1846.7
FBi(1)	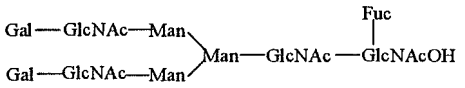	1789.7

[a] Man, mannose; Fuc, fucose; Gal, galactose; GlcNAc, *N*-acetylglucosamine.
The structure are based upon the known structure of hCG.

[b] Average mass value.

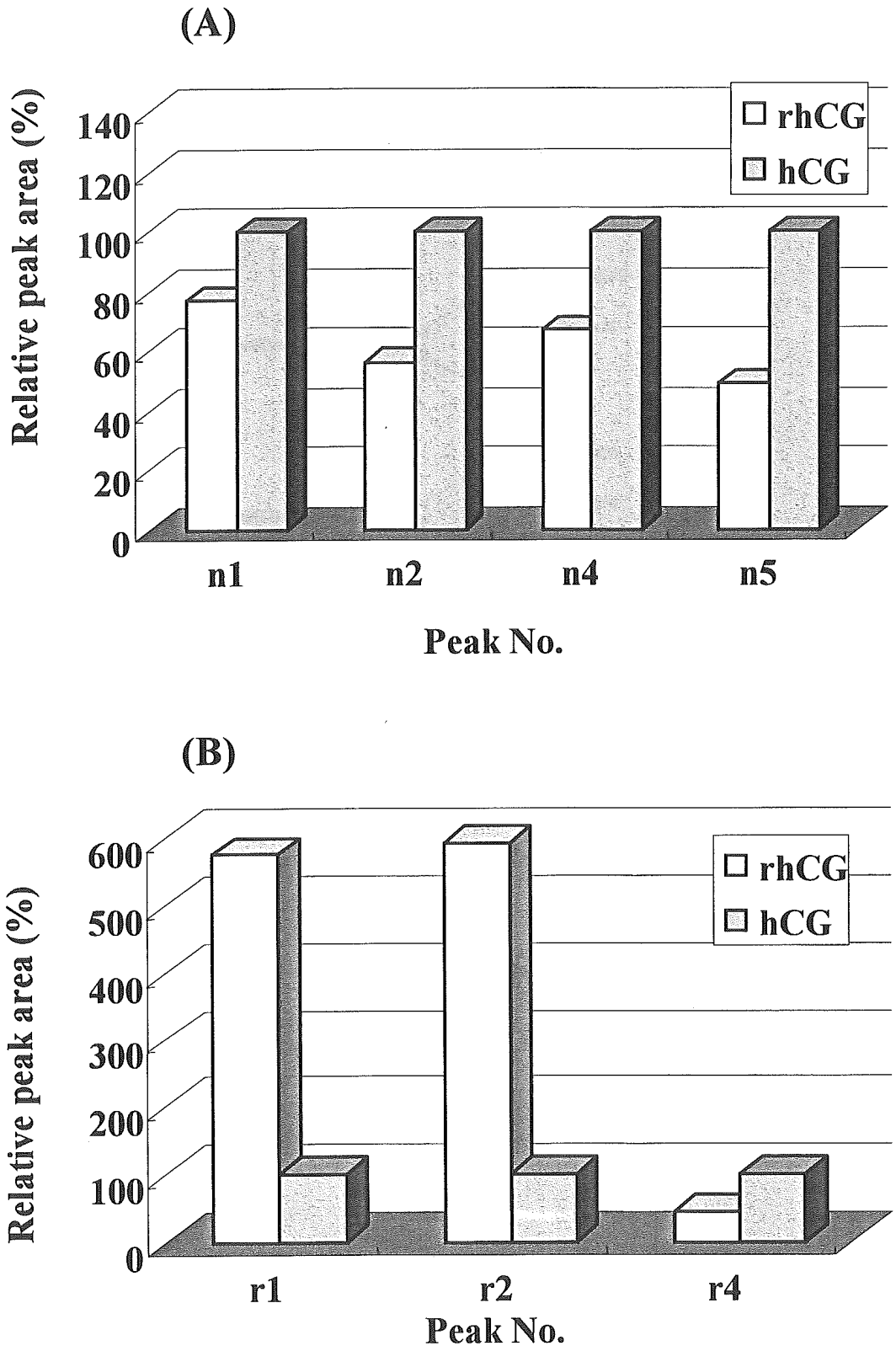

Fig. 9 rhCG及びhCGに共通して結合している糖鎖の相対結合比

(A) mono-, (B) di-sialylated biantennary

Man7/D1 :

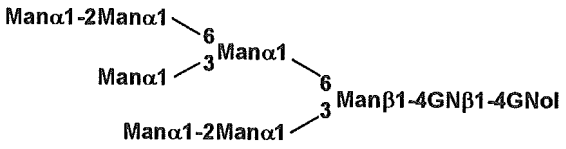

Man7/D3 :

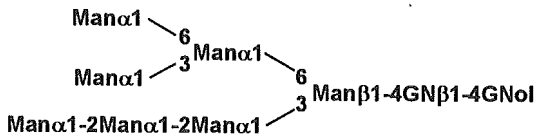

Tri :

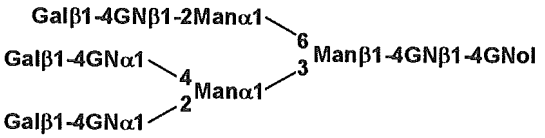

$TriNA_3$:

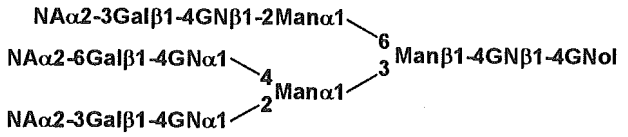

$TetraNA_4$:

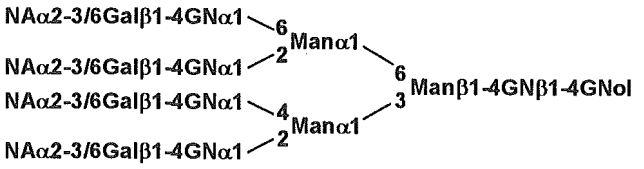

Fig. 10 モデル糖鎖の構造

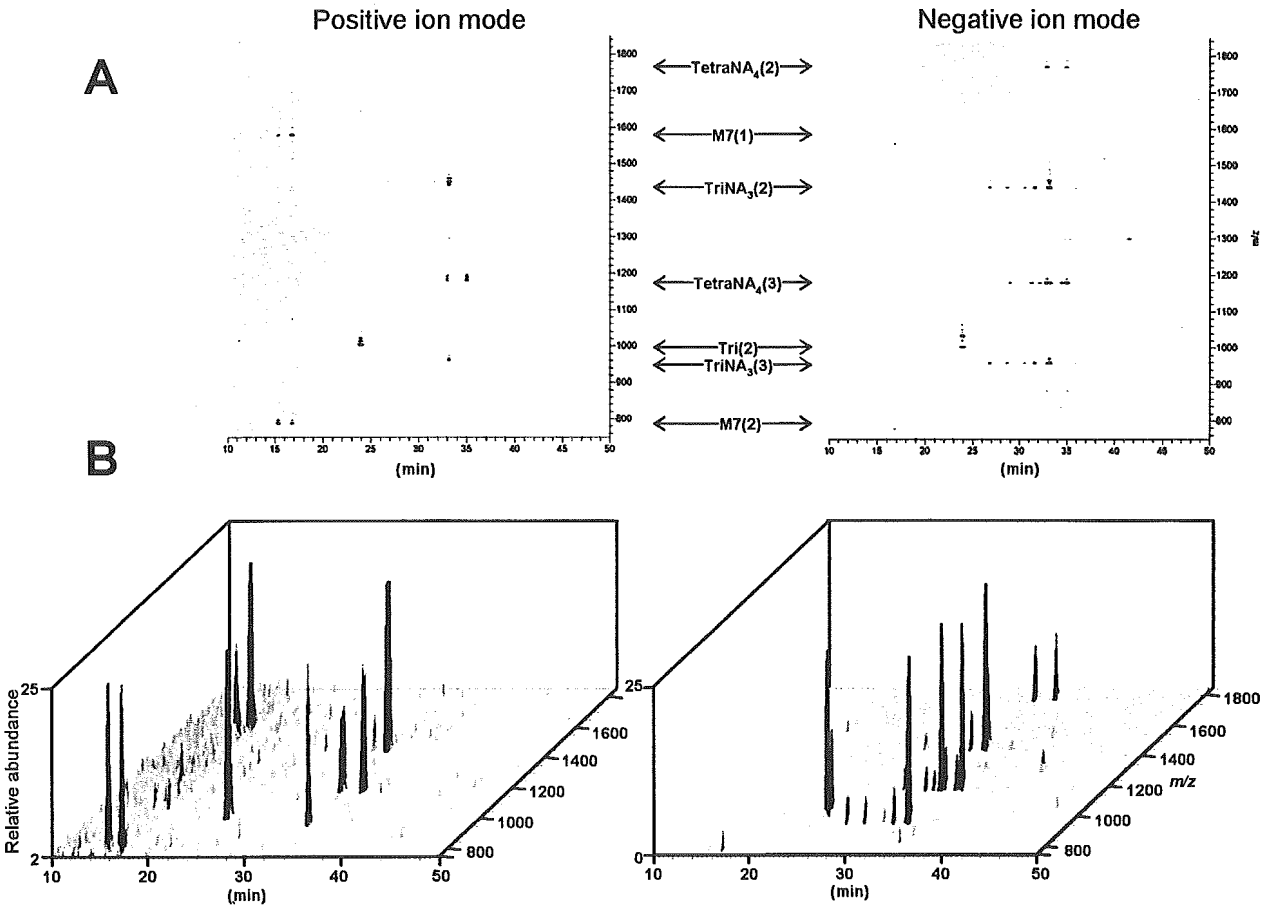

Fig.11 GCC-LC/liner ITMS-FT ICRMSによるモデル糖鎖のプロファイリング
(A) 溶出時間 vs *m/z*値、(B) 溶出時間 vs *m/z*値 vs イオン強度

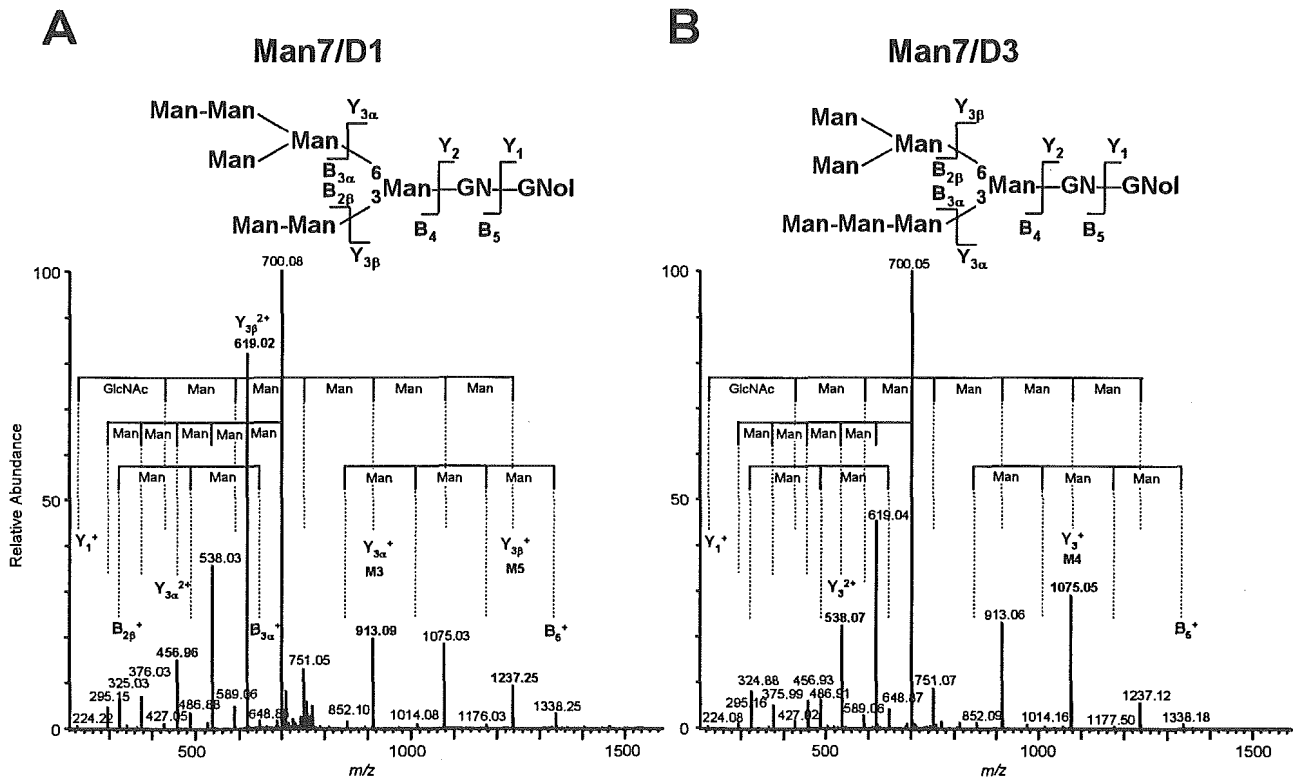

Fig. 12 高マンノース型糖鎖のプロダクトイオンスペクトル

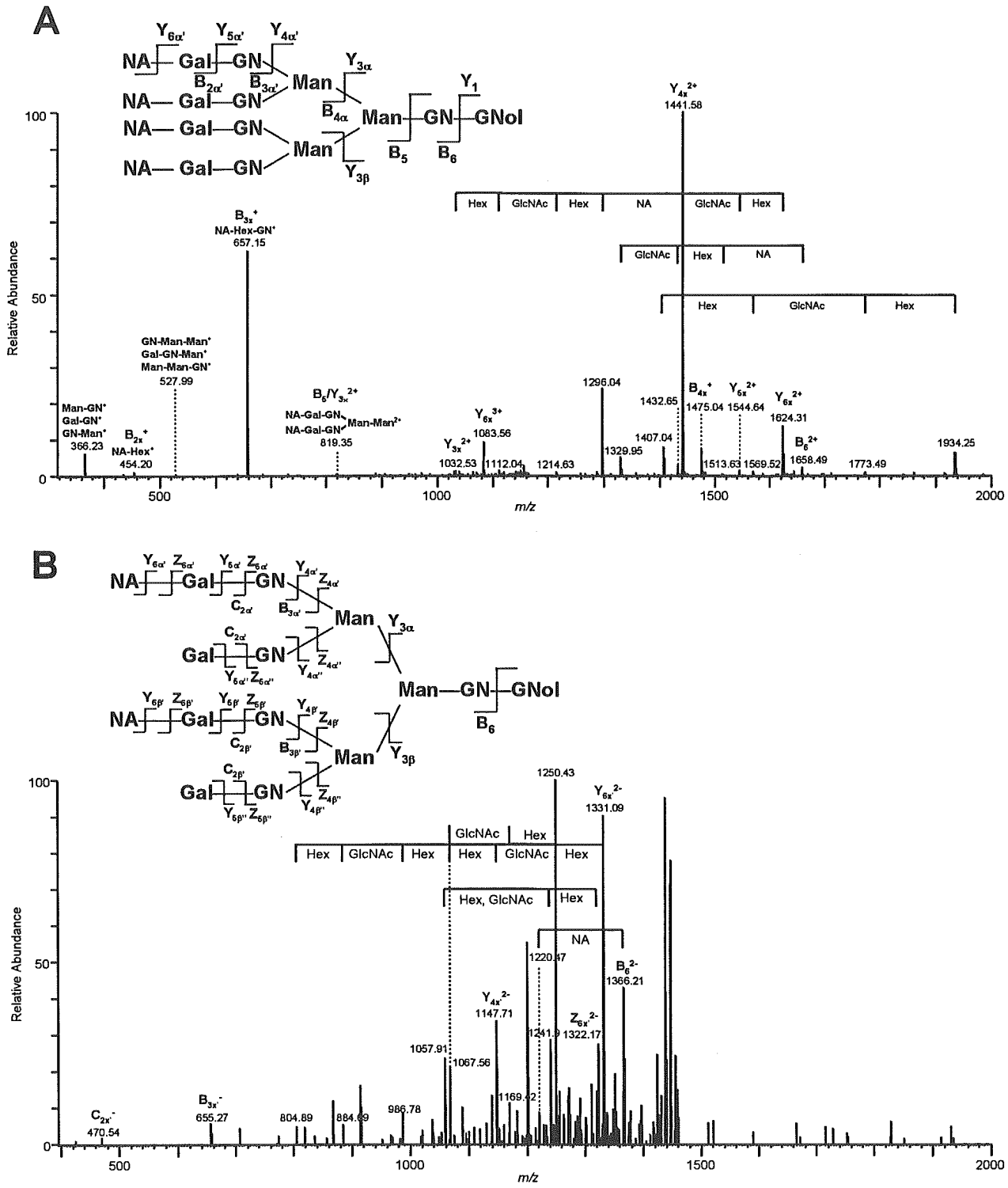

Fig. 13 シアロ糖鎖のプロダクトイオンスペクトル

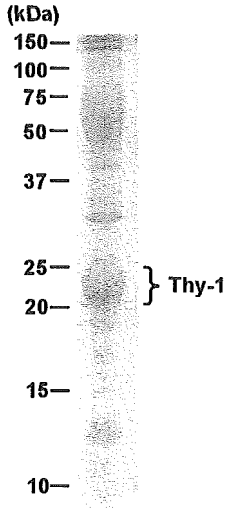

Fig. 14 ラット脳膜由来可溶性GPIアンカー型タンパク質のSDS-PAGE